Agricultural and Forest Meteorology 234–235 (2017) 127–135

Contents lists available at ScienceDirect

Agricultural and Forest Meteorology

journal homepage: www.elsevier.com/locate/agrformet

The use of weather surveillance radar and high-resolution three dimensional weather data to monitor a spruce budworm mass exodus flight

Yan Boulanger[a,*], Frédéric Fabry[b], Alamelu Kilambi[b], Deepa S. Pureswaran[a], Brian R. Sturtevant[c], Rémi Saint-Amant[a]

[a] Natural Resources Canada, Canadian Forest Service, Laurentian Forestry Centre, 1055 du P.E.P.S., P.O. Box 10380, Stn. Sainte-Foy, Québec, QC, G1 V 4C7, Canada
[b] J.S. Marshall Observatory, McGill University, MacDonald Campus, 21 111 Lakeshore Rd., Ste-Anne-de-Bellevue, Quebec, H9X 3V9, Canada
[c] Northern Resear4ch Station, Institute for Applied Ecosystems Studies, U.S. Forest Service, 5985 Highway K, Rhinelander, WI, 54501-9128, USA

ARTICLE INFO

Article history:
Received 11 August 2016
Received in revised form
22 November 2016
Accepted 23 December 2016
Available online 4 January 2017

Keywords:
Weather surveillance radar
Spruce budworm
Insect dispersal
Mass exodus flight
RUC
Insect outbreak

ABSTRACT

The likely spread of the current spruce budworm (SBW; *Choristoneura fumiferana* [Clem.]) outbreak from high to low density areas brings to the forefront a pressing need to understand its dispersal dynamics and to document mass exodus flights in relation to weather patterns. In this study, we used the weather surveillance radar of Val d'Irène in eastern Canada in combination with weather information from the Rapid Update Cycle (RUC) model output to track and document a SBW mass exodus flight that occurred on July 15–16th 2013. Analyses confirmed the potential of using weather radar and RUC data to help assess SBW mass exodus dynamics. Weather surveillance radar data suggested that the mass exodus flight originated from both the northern and southern sides of the St- Lawrence River estuary with most individuals originating from severely defoliated areas on the north shore. During the exodus flight, SBW moths may have covered a distance of over 200 km. Detailed large-scale assessment of this mass exodus flight using radar data allowed for the identification of convergence zones and a liftoff from a lightly defoliated area which has never been documented before. Based on radar and lower tropospheric weather data, SBW dispersed downwind in a rather shallow layer, probably between 400 and 800 m. These results imply that moths were generally dispersing in the vicinity of the top of the temperature inversion zone where both temperature and wind were highest throughout the exodus flight period. We advocate that the use of weather radar technology coupled with data on lower tropospheric weather conditions might benefit other monitoring tools already being used and may also help calibrate SBW atmospheric transport models.

1. Introduction

Spruce budworm (SBW) (*Choristoneura fumiferana* [Clem.]) is considered the most important pest in conifer-dominated forests of northeastern North America. Severe defoliation over several years causes significant growth reductions in the host tree (mainly balsam fir (*Abies balsamea* [L.] Miller) and white spruce (*Picea glauca* (Moench) Voss), although red and black spruce (*P. rubens* Sarg. and *P. mariana* (Mill.) B.S.P.) are also affected. Extensive mortality induced by SBW outbreaks is one of the major drivers of forest succession in balsam fir-dominated landscapes of eastern Canada (Baskerville, 1975; Bouchard et al., 2006) and has tremendous impacts on timber supply. Since ca. 2004, SBW populations have been rapidly increasing in eastern Canada. As of 2015, more than 6.3 million hectares of forest have been defoliated in the province of Quebec (Ministère des Forêts, de la Faune et des Parcs, 2016). Further spread to adjacent areas, particularly the Atlantic Region is now occurring and is expected to continue in the next few years. Potential impacts of a SBW outbreak on timber supply in Atlantic Canada might be as much as 2.4–3.3 M m^3 ha^{-1}, with direct and indirect economic losses of $10.8–$15.3 billion depending on outbreak severity (Hennigar et al., 2013). Monitoring and early detection tools are key to implement strategies to mitigate losses in areas where the outbreak might spread. For example, the early intervention strategy (Régnière et al., 2001) requires a much

* Corresponding author.
E-mail addresses: yan.boulanger@canada.ca, yan_boulanger@hotmail.com (Y. Boulanger).

http://dx.doi.org/10.1016/j.agrformet.2016.12.018
0168-1923/

better understanding of SBW spatiotemporal population dynamics including long-distance dispersal.

Long-distance dispersal is a very common feature for several insect species, including agricultural and forest pests (e.g., Westbrook et al., 1998; Chapman et al., 2003). Although this strategy incurs individual costs (Chapman et al., 2015), it may maximize survival in a spatiotemporal variable landscape by allowing offspring to move to more suitable habitats and exploit new resources (Southwood, 1977; Drake et al., 1995; Dingle and Drake, 2007). Observations made during the last major outbreak (~1965–1992) suggested that under suitable weather conditions, SBW are capable of long-distance mass exodus flights during which several millions of individuals disperse from severely defoliated areas over very large distances (Schaefer, 1976; Greenbank et al., 1980; Dickison, 1990). These dispersal events could initiate new epicenters and contribute to the fast and large scale spread of SBW outbreaks (Clark 1979). If the flight period of immigrants coincides with a local low-density population, it may increase local mating success (Miller et al., 1978; Régnière et al., 2013) and the realized fecundity of local populations so that their density exceeds a threshold above which control by natural enemies is no longer effective (Régnière et al., 2013). Long-distance dispersal events may thus contribute to regional and subcontinental synchrony in outbreak occurrence (Peltonen et al., 2002).

Assessing SBW mass exodus flight dynamics is a challenging endeavour. Indirect estimations of moth dispersal include examination of the egg-to-moth ratios (Nealis and Régnière, 2004), seasonal variations in sex ratio, wing length and dry weight of specimens (Rhainds, 2015), variation in phoretic mite load on dispersing adults, or comparisons between trap captures and SBW phenological models (Sturtevant et al., 2013). However, these techniques fail to estimate the origin, trajectory and extent of dispersal events. Aerial trapping using tethered balloons or towed nets attached to aircrafts (e.g., Greenbank et al., 1980) could be used but the cost limits the extent to which such techniques can be applied to track moth flight. Reliable tools to assess SBW exodus flight patterns are therefore needed.

High-altitude insect flight and migratory behaviour can be readily documented using radar technology (Chapman et al., 2003; Drake and Reynolds, 2012). First attempts to document the SBW long-distance dispersal behaviour using modified marine (Dickison et al., 1983) and airborne radars (Greenbank et al., 1980; Dickison et al., 1983) were successful during the last major SBW outbreak in New Brunswick. More recently, vertical looking radar (VLR) specifically designed to target insect dispersal were developed to monitor high-altitude dispersal of several insect species notably in Australia (Drake, 2002) and the United Kingdom (Chapman et al., 2003). Although these radars provide very detailed information about body orientation, altitudinal profile, velocity and identity of insect species aloft, they only look up which prevents large-scale assessment of exodus flights (Chapman et al., 2003; Drake and Reynolds 2012). This limitation also applies to older marine and airborne radars that can hardly resolve echoes beyond a few kilometers (Gauthreaux et al., 2008).

More recently, weather surveillance radar (WSR) was successfully used to track bat (Horn and Kunz 2008) and bird migration (e.g., Gauthreaux and Belser 1998; Diehl et al., 2003; Gauthreaux et al., 2008), as well as the dispersal patterns of forest (Ainslie and Jackson, 2010) and agricultural insect pests (Nieminen et al., 2000; Leskinen et al., 2011; Rennie 2014; Westbrook et al., 2014). Considering their larger spatial coverage and narrower beam widths compared to the aforementioned radars, WSR can readily detect aerial abundance, speed and direction of biological targets over areas >1000 km^2 (Westbrook and Isard, 1999). Radar reflectivity patterns can be used to determine the origin of mass exodus flights as well as their realized pathway (Westbrook et al., 2014). WSR can thus monitor mass exodus flights of SBW as they occur and track them over a large spatial extent (Chapman et al., 2003). This would benefit pest management strategies by improving our understanding of how and when these flights occur (Westbrook and Isard, 1999; Westbrook et al., 2014). Until now this technology has not been applied to track SBW mass exodus flight.

Long-distance dispersal in nocturnal insect species frequently occurs at high-altitude (from about 200 m to above 2 km) with individuals frequently concentrating within well-defined air layers in the lower troposphere (e.g., Reynolds et al., 2005; Wood et al., 2006). For instance, migrating insects have been found near the top of temperature inversion zones or within zones of subsidence inversion (Reynolds et al., 2005) where maximum horizontal wind speed is frequently recorded (Wood et al., 2006). Such a behavior may maximize groundspeed and dispersal distances (Drake et al., 1995; Reynolds et al., 2005; Chapman et al., 2011). As wind and temperature are known to vary greatly within the lower troposphere, knowledge regarding the heights of flight is thus essential to identify the air layer in which the insects are dispersing and thus to better understand their plausible flight-paths, origin and destination (Chapman et al., 2002). Previous analyses have shown that SBW in exodus flight frequently adopt a similar strategy (Greenbank et al., 1980). However, extensive lower tropospheric weather and radar data at that time were collected using airborne and ground radars that do not allow for a continuous and large-scale appraisal of SBW exodus flight vertical dynamics. Vertical density profiles of the exodus flight can be coarsely documented with WSR using reflectivity data collected at different Plan Position Indicator (PPI) angles. Furthermore, fine numerical weather simulations are now available and allow for a finer-scale three-dimensional characterization of the lower troposphere. The concurrent use of spatially extensive WSR and high-resolution three-dimensional weather data could therefore provide details on SBW dispersal dynamics.

On the night of July 15–16th 2013, a mass exodus flight of SBW was observed over various locations on the southern banks of the St. Lawrence River estuary, Québec, Canada. During this event large numbers of moths (>35 000 per trap) were collected in light traps (Rhainds 2015). Analyses that considered variations in sex ratio and moth morphology suggested that individuals might be from synchronized, pulsed emergence of local rising populations (Rhainds 2015). In the present study, our objective was to assess the ability of a WSR, namely the Val d'Irène radar, to track and document the SBW mass exodus flight that occurred that night over the Lower St. Lawrence region. More specifically, we developed a base product to monitor the horizontal movement of insects. The inspection of cleaned radar images should allow for the identification of the origins of the exodus flight as well as its density, speed and direction. We then used this product along with high-resolution 3D weather data to compare the speed and direction of the exodus flight to lower tropospheric weather conditions as well as to help assess if the altitude at which moths were dispersing was a function of tropospheric temperature and wind conditions.

2. Material and methods

2.1. Weather surveillance radars and insects

All over North America and elsewhere around the world, WSR are being used to monitor weather. This infrastructure was installed over the last few decades to detect weather and warn people and authorities of meteorological threats. Although WSR have been designed and optimized to detect precipitation, most objects can reflect the microwave pulses they transmit, and hence be detected by radar, including the ground, water surfaces and flying organisms such as birds and insects. Each type of target has a set of characteris-

tics (movement, spatial texture, vertical extent, dual-polarization signatures, etc.) that can be used to identify it or at least narrow down possibilities. Insects swarms can generally be detected and distinguished from other targets, but one must rely on external information to determine what type of insect dominates the signal. This fact and the fact that radar data are routinely collected 24/7 make WSR an interesting tool to monitor insect dispersal.

The information from WSR is not however without ambiguities. Very strong targets from the ground surface, referred to as ground clutter, often mask the much weaker echoes of insects. In the case of the Val d'Irène (XAM) radar, waves on the surface of the water of the Gulf of St. Lawrence, generally known as sea clutter, can be observed in windy conditions and have an appearance on radar that is difficult to distinguish from that of insects. Finally, because insect echoes may be confused with precipitation by inexperienced users of WSR with weather, meteorological services employ a variety of techniques to remove or hide non-meteorological echoes from publicly-available radar imagery (masking of weak echoes, removal of targets identified as being of biological origin, etc.). The proper use of radar for insect detection and quantification demands interpretation of the raw data to minimize those ambiguities as much as possible.

Information available from WSR radars include reflectivity, related to the number and size of raindrops, ice crystals or snowflakes per unit volume, the Doppler velocity, or whether the target appears to be moving towards or away from the radar, and, increasingly, dual-polarization information providing some clues about target shapes (this latter information is not yet available from the XAM radar). The scanning strategy of WSR implies that echoes are assessed at different altitudes all around the radar, while periodic revisits are made to monitor the rapid evolution of severe weather. To monitor the targets around the radar at multiple altitudes, several scans are made at different elevation angles. In Canada (Joe and Lapczak, 2002), WSR use 24 elevation angles completed in five minutes to assess the weather around the radar. But because these fast scans are not ideal to measure Doppler velocity or to clean ground targets, another set of slowly-rotating scans at four elevation angles are added in the next five minutes to better measure velocity and to get rid of stationary ground targets. Even if both reflectivity and Doppler velocity are measured at these four angles, we refer to them here as the Doppler scans. This scanning strategy shapes what data are available for insect monitoring: every 10 min, we obtain reflectivity information at many angles for reflectivity, but that information may be contaminated by ground targets; then we have a few scans with velocity information that is cleaned from ground targets but also has less sensitivity. Our analysis of insect coverage and dispersal hence uses a combination of the more sensitive and higher coverage reflectivity scans blended with the cleaned Doppler scans.

2.2. Data source

The key data source used in this study is the XAM radar (48.48 N, 67.60 W) of Environment Canada (Fig. 1). Located at 710 m altitude, the radar covers the southern and northern sides of the St. Lawrence estuary as well as northern New Brunswick. The first advantage of using this radar is obviously its proximity with the area currently defoliated by spruce budworm in eastern Quebec. Furthermore, being located on a hilltop, this radar is one of the very few in Canada that perform scans at elevations lower than the horizon. This peculiarity improves our ability to detect insects that are commonly flying low (below 1000 m, Greenbank et al., 1980) up to distances often exceeding 120 km from the radar. It also has a narrow beam width of 0.65°, which further increases its sensitivity to weak echoes and allows us to get a few independent height measurements at altitudes of migrating insects.

2.3. Image processing

Our first task was to develop a base product to monitor the horizontal movement of insects. Our goal was to make a map of the maximum reflectivity observed by radar at low elevations that can be attributed to insects or precipitation, taking into advantage the fact that no precipitation was observed that night. What should be done would be to identify pixels contaminated by ground targets, mask them, and pick for each range and azimuth the strongest unmasked reflectivity remaining at low elevations. What would be a relatively simple process in many countries is complicated by the peculiarities of the Canadian radars' scanning strategy: we have at our disposal a combination of sensitive scans at 24 elevation angles that are ground clutter contaminated, and of less sensitive scans at only 4 low elevation angles that are mostly free of ground targets. We hence generated our base product as follows. We considered only data from the five lowest higher-sensitivity unfiltered scans (−0.5°, −0.3°,−0.1°, 0.1°, and 0.3°) and from the three lowest lower-sensitivity clutter-filtered scans (long range −0.5°, short range −0.5°, and short range −0.2°). The first step was to create a scan by taking the maximum reflectivity of the five lowest higher sensitivity unfiltered scans. This process fills in the shadow areas affected by beam blockage at lower elevation scans with the data from the higher elevation scans. The clutter pixels in this unfiltered scan are identified by an average clutter mask determined during clear weather, and replaced by the maximum of three lowest clutter-filtered less sensitivity scans. Furthermore, high reflectivity values (greater than 25 dBZ) with low echo tops (lower than 2.5 km) in the clutter mask areas are considered to be unfiltered ground targets and are replaced by an average of the reflectivity values from the immediate neighborhood. Because insect density tends to be higher closer to the surface, the peak reflectivity among a set of angles is generally from the lowest angle, unless that angle is contaminated by clutter or affected by beam blockage.

2.4. Regional defoliated areas

At the time of the SBW mass exodus flight in 2013, a total of 3.2 million ha were defoliated in the Quebec province with most of the defoliation concentrated in the North Shore (2 465 721 ha) where it was mostly severe (Ministère des Forêts, de la Faune et des Parcs, 2016, see also Fig. 1). On the south side of the estuary, 117 580 ha were defoliated, mostly lightly, in areas concentrated near the coast and along the Matapedia Valley (Fig. 1).

2.5. Weather conditions

Lower tropospheric wind speed, wind direction and temperature profiles over the study area for the 24 h period beginning at 1600 UTC (1200 EDT) July 15th were retrieved from the Rapid Update Cycle (RUC) operational weather prediction system.[1] Hourly RUC weather data were further downscaled to a 10-km grid snapped to the extent of the study 236 area using BioSIM v11.0.3.6 (Régnière and St-Amant, 2007; Régnière et al., 2014). BioSIM interpolate hourly temperatures (°C), precipitation (mm), relative humidity and wind speed by matching georeferenced sources of weather data (here the RUC dataset) to spatially georeferenced points (the 10-km grid), adjusting the weather data for differences in latitude, longitude, and elevation between the source

[1] Accessed from http://nomads.ncdc.noaa.gov/data.php.

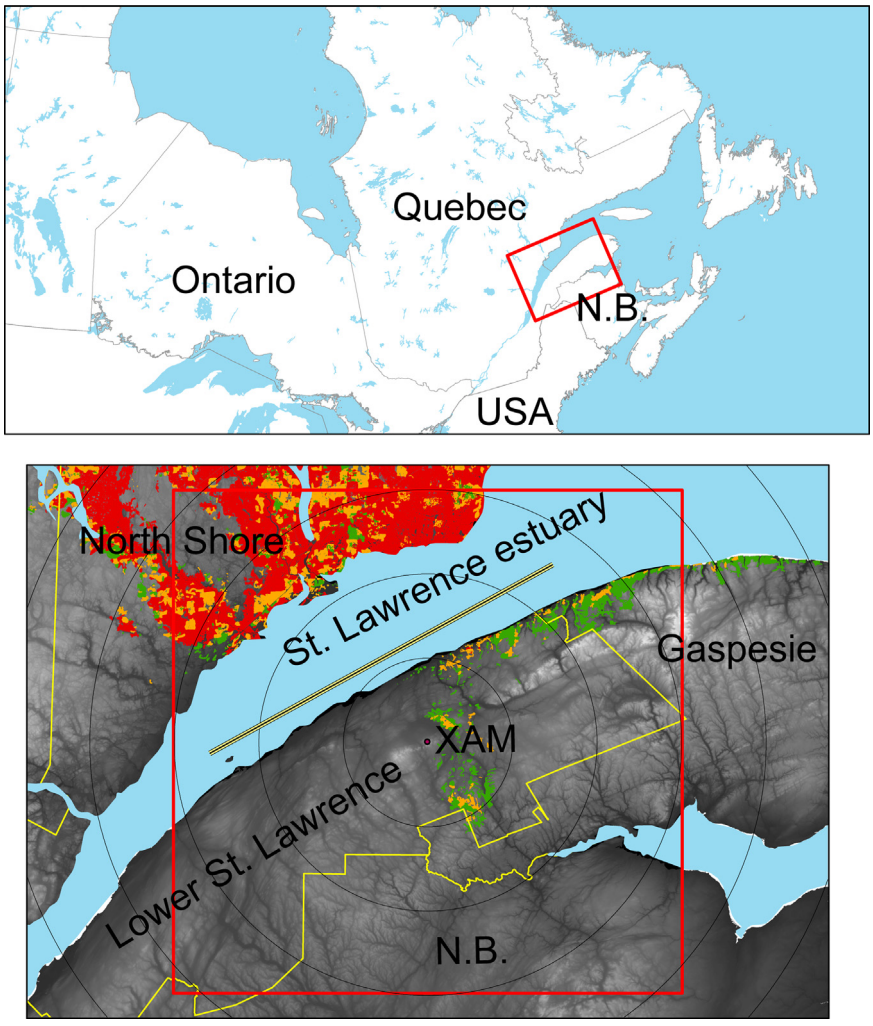

Fig. 1. Topography and location of the area considered for WSR data analyses (red square) as well as the position of the XAM radar. Also shown is the transect location (yellow-highlighted black line) above which detailed vertical profile WSR data and lower tropospheric weather data were collected. Equidistant circles represent 40-km distance increase from the XAM radar. Administrative regions are delineated in yellow. Defoliated areas in 2013 are also shown (green: light defoliation, orange: moderate defoliation; red: severe defoliation). N.B.: New Brunswick. (For interpretation of the references to colour in this figure legend, the reader is referred to the web version of this article.)

of weather data and each grid cell location by spatial regressions. Weather parameters were retrieved at the centroid of each grid cell at a 200-m interval for heights between 0 and 2000 m above ground level (agl).

2.6. Analyses

2.6.1. Reflectivity chronology

Filtered radar images were assessed at a 10-min interval and 1-km resolution to monitor potential insect echoes reflectivity and radial velocity from July 15th 1700 EDT (2100 UTC) to July 16th 0600 EDT (1000 UTC). Detailed reflectivity and velocity analyses were limited to a 240 × 240 km zone centered on the XAM WSR (Fig. 1). A reflectivity chronology was built using the 10-min interval data to visually assess the origin, density and pathways of the potential exodus flight.

2.6.2. Vertical density profile in relation with lower tropospheric weather conditions

Vertical reflectivity profiles were retrieved for a specific transect section over the St. Lawrence estuary (Fig. 1) to help assess variations in the density of moths at various altitude over the time period considered. This location was selected to minimize contamination from residual ground clutter and because it is at ranges where the radar scans the lowest. As distance to the XAM WSR radar varied along the transect, vertical resolution varies from about 150 m at the closest point to the radar (45 km range) to about 350 m at both transect extremities (103 km range). Reflectivity altitudinal profile data were then rescaled at a 250 m resolution for display. Temperature and wind speed from the downscaled RUC data were retrieved every 10 km along this transect for 0–2000 m above ground level at 200-m interval. Contours were interpolated using the *filled.contour* function of the *graphics* package in R 3.2.4 (R Core Team, 2016). SBW vertical density profiles along the transect were then compared to the selected weather parameters.

2.6.3. Comparison between target and lower tropospheric wind radial velocities

We also used the information from radar to assess the direction and speed of insects over time. Although speed and heading of targets can be somewhat qualitatively assessed by inspecting temporal changes in short-interval reflectivity time series, WSRs do not directly provide true echo ground speed and direction. Rather, WSRs measure the component of the velocity of the target in the radial direction towards or away from the radar using Doppler principles. Target radial velocity was compared with lower tro-

pospheric downscaled wind speed and direction between 0 and 2000 m above ground level at 200 m intervals. For this comparison, wind direction and speed from all 10-km pixels were transformed to expected radial velocity. Because RUC winds are hourly, only the first radar velocity image of the hour was used for these analyses. Radar radial velocity data over the whole study area was averaged at the same 10-km grid spacing used for lower tropospheric winds to avoid pseudoreplication. Residual radial velocity of the targets, i.e., the radial velocity of the targets relative to wind radial velocity, was then computed at the selected altitude and averaged for the whole period considered.

3. Results

3.1. Cleaned radar data chronology

We successfully retrieved echoes in clutter areas (both suppressed and not suppressed) by using information from multiple elevation angles. Blocked sectors, such as WSW of the radar however remained blocked, and good observations were impossible in these sectors (Fig. 2). Some ground targets could not be suppressed properly south and east of the radar (Fig. 2a). Weak echoes (less than −1 dBZ, Fig. 2a) presumably caused by surf over the St. Lawrence estuary and daytime insects or other biological targets primarily near the radar, were observed before 1900 EDT (2300UTC). Large areas with reflectivity exceeding −1 dBz were observed from 1900 EDT, peaking around 0000 EDT and then gradually dissipating until sunrise ∼0400 EDT (∼0800 UTC) (Fig. 2). Three distinct groups of moving targets (hereafter "waves") originating from both the northern and the southern sides of the estuary were discernible on the radar images (Fig. 2). Plume-shaped echoes (hereafter the "initial wave", W1) first appeared in early evening at 1900 EDT (2300 UTC) (Fig. 2b) primarily over defoliated areas on the northern side of the estuary and started travelling SSE over the St. Lawrence estuary. Much stronger echoes (hereafter the "main wave", W2) emerged from the NW of the study area just after sunset 2120 EDT (0120 UTC), having a reflectivity roughly 30 times stronger than the initial wave (Fig. 2c). In parallel, smaller groups of echoes (hereafter the "southern wave", W3) having a slightly weaker reflectivity than the main wave took off over defoliated areas in the Lower St. Lawrence and the Gaspe Peninsula (Fig. 2c).

In parallel, radar images allowed the identification of a thin line of enhanced echoes (CZ), initially (1900 EDT) NNE of the radar at 100 km range, moving to the SW (Fig. 2b). This line preceded a shift in target heading which occurred along a NE to SW axis. Readers can refer to Supplementary material S1 and S2 for detailed animated figures showing the 10-min interval spatially explicit chronology of cleaned radar reflectivity and radial velocity data.

3.2. Vertical density profile

Because of lack of data, we were unable to resolve echoes in the lower 250 m above the surface. The vertical density profile analysis shows that echoes were primarily concentrated below 800 m asl above the estuary (Fig. 2). Lighter echoes were recorded up to 2200 m. The top margins of echoes gradually increased up to 1500 m at 2230 EDT, stabilized and then slightly decrease in altitude after 0000 EDT with the passage of the different target waves over the transect. Echo strength was generally higher in the lower layers and generally declined with altitude regardless of the time period (Fig. 2).

3.3. Movement of targets and comparisons with lower tropospheric weather conditions

A gradual strengthening of temperature inversion occurred above the estuary after sunset, peaking around 2000 EDT, with the top of the temperature inversion zone lying at 600–800 m (Fig. 3a). Although winds were generally stronger at higher altitudes (>1500 m) before 1900 EDT, winds gradually became strongest between 400 and 1000 m for the rest of the night (Fig. 3b). The first visual comparison between reflectivity time series and winds suggested that targets were mostly moving in accordance with lower tropospheric wind above 400m. Indeed, winds in shallower layers were generally blowing in different directions compared to the apparent dispersal of targets (Supplementary material S3). Differences between the target and wind radial velocities (residual radial velocity) were lowest when considering winds between 400 and 800 m with median values varying between 2.5 and 3.5 km h^{-1} (Fig. 4). Residual radial velocity variance was also lowest when considering winds blowing at these altitudes.

4. Discussion

This study is the first to assess, and confirm, the usefulness of WSR to document SBW mass exodus flight dynamics. Similar conclusions were reached in other studies in which WSR was used to help track agricultural (Nieminen et al., 2000; Leskinen et al., 2011) and forest pests (Ainslie and Jackson, 2010). The concomitant use of lower tropospheric weather data brought further insights on the dispersal pattern of SBW. We relied on a qualitative approach rather than considering thorough statistical techniques to illustrate the potential impacts of lower tropospheric weather conditions on a mass exodus flight of SBW. This study should thus be considered as exploratory, and as such, future work is needed to thoroughly document the variation in the SBW mass exodus flight dynamics. Yet, we believe that continuous and real-time monitoring (e.g., Leskinen et al., 2011) of SBW mass exodus events using WSR and semi-automatic algorithms (Gauthreaux and Belser, 2003) might contribute to forecast and "now cast" mass exodus flights thereby helping to focus monitoring and eventually spraying to control rising SBW populations in specific areas. A similar strategy using WSR was also recently proposed to alert crop producers and pest managers for potential risks of infestation by the corn earworm moth in southern Texas, USA (Westbrook et al., 2014). WSR should thus be considered as a valuable complementary tool to others that are already applied to monitor and model SBW dispersal. Sturtevant et al. (2013) developed a SBW atmospheric transport model (SBW-ATM) based on aerobiological principles to examine the exodus flight patterns of SBW. Currently, the model is being parameterized using the biological information recorded in the 1970's by Greenbank et al. (1980). WSR data coupled with lower tropospheric weather conditions should greatly help for further calibration and validation of the model.

4.1. Limitations

WSR data are indirect tools to monitor mass insect migration and dispersal events and as such, we acknowledge that it is impossible to assert with certainty that targets were dispersing SBW individuals. However, several clues strongly supported this assumption. Vertical density profile analyses showed that most targets were concentrated below 1 km agl. Such a shallow echo is in sharp contrast with most precipitation echoes; except for drizzle, rain echoes, especially in summer, extend vertically at least up to 6 km altitude, making them easy to distinguish from biological echoes, including those from insects (Browning et al.,

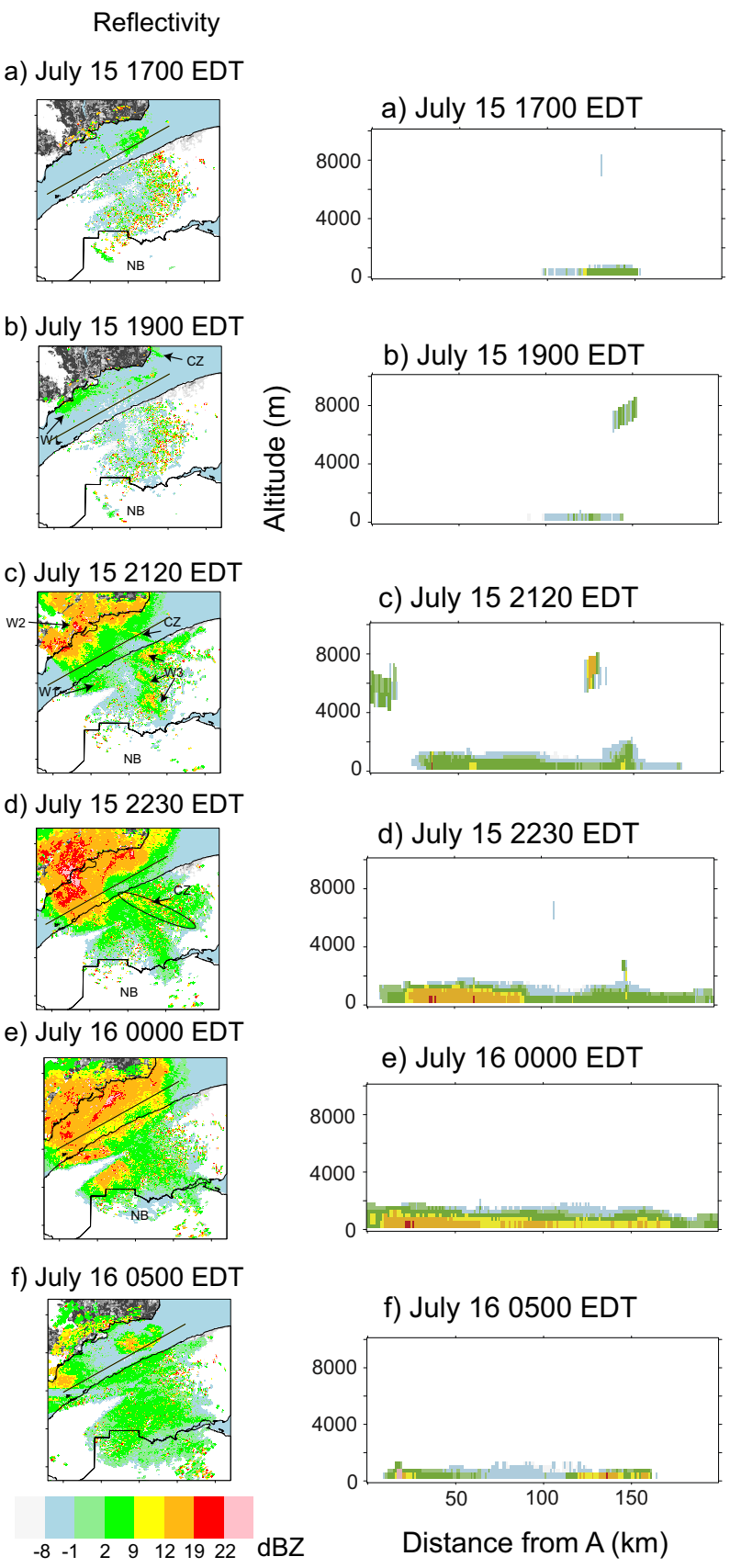

Fig. 2. Reflectivity maps (left), and altitudinal profile of reflectivity over the transect (right), for selected time periods: a) 1700 EDT; b) 1900 EDT; c) 2120 EDT; d) 2230 EDT; e) 0000 EDT; f) 0500 EDT. The transect position is illustrated on reflectivity maps by a black line above the estuary. Apparent take-offs and dispersal for each of the three waves (W1, W2, W3) are identified on the specific reflectivity maps. A thin higher-reflectivity line potentially associated with a wind convergence zone (CZ) is also identified. Defoliated areas in 2013 are also shown. See Fig. 1 for defoliation classes and abbreviations.

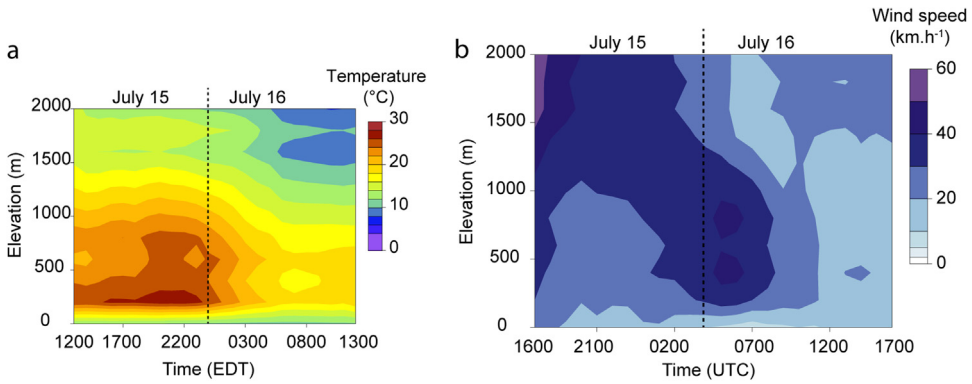

Fig. 3. Temperature (a) and wind speed (b) vertical profile above the transect as assessed from the RUC numerical model. Values were averaged along the transect at a specific altitude and time period (EDT). The vertical dashed line refers to midnight EDT July 16.

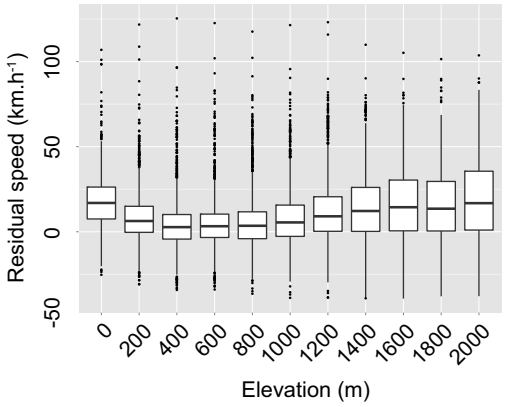

Fig. 4. Boxplot showing the differences between target and wind radial velocities (=residual radial velocity, in km h^{-1}) when considering winds blowing between 0 and 2000 m at 200 m interval.

2011; Fabry, 2015). Furthermore, no precipitation was reported in the area such as at the Mont-Joli weather station2 despite a prolonged 4-h period with echoes stronger than 10 dBZ that should have been sufficient to be associated with observable precipitation (Supplementary material S1). We also acknowledge that discriminating SBW exodus flight from other biological targets might be problematic (Martin and Shapiro, 2007; Gauthreaux et al., 2008). However, the time of the year as well as the rather low potential airspeed of targets helped to discriminate echoes with migrating birds (Gauthreaux et al., 2008). The night we investigated (July 15–16 2013) coincided with peak male moth flight activity, estimated using the insect phenology model BioSIM. The timing of mass echoes is also highly consistent with published studies of SBW liftoff (Henson, 1951; Greenbank et al., 1980). To our knowledge, no other insects in this area might have shown similar population density during this time frame. Forthcoming implementation of dual-polarization capabilities for the existing WSR network in Canada should further improve the ability to better resolve and track insect echoes (Chapman et al., 2011; Melnikov et al., 2014).

4.2. Origins of the exodus flight

WSR data suggested that the July 15–16th mass exodus flight originated from both the northern and southern sides of the estuary with most individuals coming from the severely defoliated areas of the North Shore (contrast Fig. 1 with Fig. 2c at 2020 EDT). Although it is impossible to determine the actual flightpath of individual moths using WSR, echo patterns suggested SBW moths originating from this area might have travelled distances over 200 km at speeds sometimes reaching more than 50 km h^{-1} (Supplementary material S2). A north shore origin of the mass exodus flight contradicts Rhainds' (2015) speculations based on light trap captures and body size measurements and his recent conclusions stating that the great majority of the thousands of SBW individuals collected in light traps on the southern side of the estuary were from synchronized, pulsed emergence of local populations instead of distant dispersers. Rhainds (2015) conclusions build on a limited body of literature referring to mass SBW exodus flights. Variations in sex ratio (Rhainds and Heard, 2015) and moth morphology (Rhainds and Brodersen, 2012) suggested a local origin for the trap catches. Whether the July 15–16th 2013 mass exodus event was the exception rather than the rule in this regard remains unknown. In any case, this calls for a much better integration of WSR data monitoring with existing collection methods in order to improve our understanding of the SBW dispersal dynamics. Detailed large-scale assessment of this mass exodus flight using WSR data allowed for the identification of peculiar dispersal patterns that might have been overlooked using traditional monitoring tools. Two of these patterns are worth mentioning. First, apparent liftoff from lightly to moderately defoliated areas on the southern side of the estuary suggests that mass exodus flights (at least in moth densities that are observable by WSR), might originate from areas where severe resource depletion may have not yet occurred. This dispersal pattern contrasts with Greenbank (1973) who stated that female moth emigration might be a function of population density since food depletion in the larval stage would produce females that are lighter and hence are more likely to disperse. Whether such exodus flight is an example of "preemptive" dispersal (Dingle and Drake 2007) needs further investigation. Indeed, emigrating moths from these lightly infested areas might actually be the previous day's immigrants from more severely defoliated areas as moths can make more than one dispersal flight and stop while in transit (Greenbank et al., 1980). More complete analyses of mass exodus flights for the entire flight period are therefore required to address this question.

4.3. Identification of particular SBW dispersal patterns using WSR

Alongside, WSR allowed for the identification of a potential convergence zone associated with a lower-tropospheric wind shift over the estuary that may have contributed to the enormous moth deposition on the southern side of the estuary. A thin line of higher radar reflectivity travelling from the NE to the SW over the estuary was indeed observed which was followed by an important wind shift above 200 m. Very high densities of SBW moths observed at ground-level have most often been attributed to the passage of cold fronts, thunderstorms and rainstorms due to mesoscale wind convergence and updraft (Henson 1951; Greenbank et al., 1980;

Dickison et al., 1983; Dickison et al., 1986). Such observation might imply that wind shift-induced convergence and moth deposition may also take place during fair weather. Mass moth deposition at low density sites has been hypothesised to contribute to population growth by gravid immigrant females laying eggs after arrival or by immigrant males enhancing local mating success (Régnière et al., 2013). If this happens, new "hot-spots" or epicentres" could be triggered contributing to the spread of outbreaks (Clark 1979). Further characterization of these fair-weather wind convergence zones are needed as these events could have implications for pest management, particularly to use "early intervention" and target potential "hot-spots".

4.4. SBW dispersal in relation to lower tropospheric weather conditions

WSR data suggested that SBW dispersed downwind in a rather shallow layer. Recent analyses have shown that strong directional dispersal in SBW was enhanced by prevailing wind direction during periods of active flight (Anderson and Sturtevant 2011). The very low discrepancies between wind and moth radial velocities at specific altitudes suggest that individuals made a rather small contribution to their horizontal displacement speed (Aralimarad et al., 2011; Chapman et al., 2011, 2016). Rather, moths seemed to mostly drift with lower tropospheric winds, with sharp changes in wind direction triggering a prompt response in moth heading. Given several limitations, it was impossible to assess from WSR data if targets were evenly distributed or concentrated at specific levels within this shallow layer: weather radars have limited angular resolution (half-power beam width of 0.65°); they make measurements at a low number of partially overlapping elevation angles; and, the large distances to the targets of interest (50–100 km) leads to vertical smearing and blockage of the lowest levels due to the curvature of the Earth. As a result, it is very difficult to say more than insects tend to be more concentrated in the bottom than in the top of the lowest kilometer of the atmosphere. Exodus flight within this lower tropospheric layer is in accordance with previous observations from ground- and airborne Doppler radars which routinely recorded considerable SBW moth densities between 100 and 1000 m agl, with abundance usually peaking at mid-elevation, i.e., generally between 300 and 800 m (Greenbank et al., 1980; Dickison et al., 1983, 1986). Similar cruising altitudes were recorded for seasonal migrating nocturnal Lepidoptera (e.g., Wood et al., 2006, 2009; Chapman et al., 2008, 2016; Reynolds et al., 2008; Aralimarad et al., 2011).

Analyzing lower tropospheric wind data gave further insights regarding in which specific layers moths were more likely to disperse. Lower residual radial velocity value and lower variance between 400 and 800 m should be a valuable indication that most individuals were dispersing within this specific layer. Indeed, dispersal below 400 m is unlikely as this would imply a median residual radial velocity above 10 km h^{-1}, an airspeed unlikely to be reached by the SBW (expected to reach 7.2 km h^{-1}; Greenbank et al., 1980; Sturtevant et al., 2013). Recall that the true moth velocity vector cannot be determined from WSR data as the true orientation is unknown. As such, residual radial velocity necessarily underestimates the actual air speed unless the moth orientation is truly radial relative to the radar. Data also suggested that there may be large discrepancies between wind direction outside the 400–800 m range and the apparent movement of targets (Supplementary material S3). These results would imply that moths were generally dispersing in the vicinity of the top of the temperature inversion zone where both temperatures and wind were highest throughout the exodus flight period. Dispersal near the top of temperature inversion zones has already been observed for several nocturnal migrating insects (Chapman et al., 2003; Reynolds et al., 2005, 2008; Wood et al., 2006, 2010; Aralimarad et al., 2011; Rennie, 2014), especially in temperate regions (Wood et al., 2006, 2010; Chapman et al., 2011). One might hypothesize that such a downwind dispersal pattern, presumably within the warmest and windiest layers of the lower troposphere is the result of an evolved strategy that contribute to increase flight performance and migration distances (Wood et al., 2010; Chapman et al., 2008, 2016) rather than passive dispersal dynamics similar to wind-drifted particles. Yet, further analyses involving vertical looking radars are required to determine if SBW mass exodus events are related to specific lower tropospheric conditions that maximize insect dispersal distances.

5. Conclusions

Our analyses confirm the potential of WSR to help assess SBW mass exodus events. The usefulness of WSR to track dispersal of insect pest species has been recently recognized (Leskinen et al., 2011; Westbrook et al., 2014). Inexpensive computing power used to analyze WSR digital data (Ruth et al., 2008) now allows for a much better broad scale assessment of these events when compared to the radar tools that were first developed during the last major outbreak. Since then, several improvements have been made to the existing weather radar surveillance network worldwide including a recent increase in the number of units and great advances regarding their sensitivity and stability (Joe and Lapczak 2002). Combining data from various WSR (Gauthreaux and Belser 1999; Kelly et al., 2012), including selected NEXt-generation RADars (commonly known as NEXRADs) in northeastern United States could further increase the spatial coverage for which SBW dispersal could be monitored. Yet, the efficiency of other WSR to detect SBW mass exodus flight has to be further explored. The use of finer grid lower tropospheric weather data (3-km RApid Refresh [RAP] data) would also help to identify finer atmospheric patterns impacting SBW high altitude dispersal. These analyses would allow for a much better appraisal of past but also future SBW dispersal events.

Acknowledgements

We are grateful to Environment Canada which provided the XAM weather surveillance radar raw data to be analyzed. NOAA provided the RUC weather data. Jean-Martin Lussier (CFS), Pierre Vaillancourt (EC) and Louise Bussières (EC) offered valuable comments and suggestions in the initial phases of this project. Jacques Régnière (CFS), Joseph Charney (USFS), Gary Achtemeier (USFS retired) as well as two anonymous referees gave useful comments on previous versions of the manuscript. Funding was provided by the Canadian Forest Service.

Appendix A. Supplementary data

Supplementary data associated with this article can be found, in the online version, at http://dx.doi.org/10.1016/j.agrformet.2016.12.018.

References

Ainslie, B., Jackson, P.L., 2010. Investigation into mountain pine beetle above-canopy dispersion using weather radar and an atmospheric dispersion model. Aerobiologia 27, 51–65.

Anderson, D.P., Sturtevant, B.R., 2011. Pattern analysis of eastern spruce budworm *Choristoneura fumiferana* dispersal. Ecography 34, 488–497.

Aralimarad, P., Reynolds, A.M., Lim, K.S., Reynolds, D.R., Chapman, J.W., 2011. Flight altitude selection increases orientation performance in high-flying nocturnal insect migrants. Anim. Behav. 82, 1221–1225.

Baskerville, L.G., 1975. Spruce budworm: super silviculturist. For. Chron. 51, 138–140.

Bouchard, M., Kneeshaw, D., Bergeron, Y., 2006. Forest dynamics after successive spruce budworm outbreaks in mixedwood forests. Ecology 87 (9), 2319–2329, http://dx.doi.org/10.1890/0012-9658.
Browning, K.A., Nicol, J.C., Marsham, J.H., Rogberg, P., Norton, E.G., 2011. Layers of insect echoes near a thunderstorm and implications for the interpretation of radar data in terms of airflow. Q J R Meteorol Soc. 137, 723–735.
Chapman, J.W., Reynolds, D.R., Smith, A.D., Riley, J.R., Pedgley, D.E., Woiwod, I.P., 2002. High-altitude migration of the diamondback moth *Plutella xylostella* to the U.K.: a study using radar, aerial netting and ground trapping. Ecol. Entomol. 27, 641–650.
Chapman, J.W., Reynolds, D.R., Smith, A.D., 2003. High-altitude insect migration monitored with vertical-looking radar. Bioscience 53, 503–511.
Chapman, J.W., Reynolds, D.R., Mouritsen, H., Hill, J.K., Riley, J.R., Sivell, D., Smith, A.D., Woiwod, I.P., 2008. Wind selection and drift compensation optimize migratory pathways in a high-flying moth. Curr. Biol. 18, 514–518.
Chapman, J.W., Drake, V.A., Reynolds, D.R., 2011. Recent insights from radar studies of insect flight. Ann. Rev. Entomol. 56, 337–356.
Chapman, J.W., Reynolds, D.R., Wilson, K., 2015. Long-range seasonal migration in insects: mechanisms, evolutionary drivers and ecological consequences. Ecol. Lett. 18, 287–302.
Chapman, J.W., Nilsson, C., Lim, K.S., Bäckman, J., Reynolds, D.R., Alerstam, T., 2016. Adaptive strategies in nocturnally migrating insects and songbirds: contrasting responses to wind. J Anim. Ecol. 85, 115–124.
Clark, W.C., 1979. Spatial structure relationship in a forest insect system: simulation models and analysis. Bull. Soc. Entomol. Suisse 52, 235–257.
Dickison, R.B.B., Haggis, M.J., Rainey, R.C., 1983. Spruce budworm moth flight and storms: case study of a cold front system. J. Clim. Appl. Meteor. 22, 278–286.
Dickison, R.B.B., Haggis, M.J., Rainey, R.C., Burns, M.D., 1986. Spruce budworm moth flight and storms: further studies using aircraft and radar. J. Clim. Appl. Meteor. 25, 1600–1608.
Dickison, R.B.B., 1990. Detection of mesoscale synoptic features associated with dispersal of Spruce Budworm moths in eastern Canada. Phil. Trans. R Soc. Lond. B 328, 607–617.
Diehl, R.H., Larkin, R.P., Black, J.E., 2003. Bird migration around the Great Lakes on Doppler radar: implications for habitat conservation. Auk 120, 278–290.
Dingle, H., Drake, V.A., 2007. What is migration? Bioscience 57, 113–121.
Drake, V.A., Reynolds, D.R., 2012. Radar Entomology: Observing Insect Flight and Migration. CABI, Wallingford, UK.
Drake, V.A., Gatehouse, A.G., Farrow, R.A., 1995. Insect migration: a holistic conceptual model. In: Drake, V.A., Gatehouse, A.G. (Eds.), Insect Migration:Tracking Resources Through Space and Time. Cambridge University Press, Cambridge (United Kingdom), pp. 427–457.
Drake, V.A., 2002. Automatically operating radars for monitoring insect pest migrations. Insect Sci. 9, 27–39.
Fabry, F., 2015. Radar Meteorology – Principles and Practice. Cambridge University Press, Cambridge, UK.
Gauthreaux, S.A., Belser, C.G., 1998. Displays of bird movements on the WSR-88D: patterns and quantification. Weather Forecast 13, 453–464.
Gauthreaux, S.A., Belser, C.G., 1999. Bird migration in the region of the Gulf of Mexico. In: Slotow, R.H., Adams, N.J. (Eds.), Proc 22 Int Ornithol Congr, Durban. Johannesburg : BirdLife South Africa, pp. 1931–1947.
Gauthreaux Jr, S.A., Belser, C.G., 2003. Radar ornithology and biological conservation. Auk 120, 266–277.
Gauthreaux, S.A., Livingston, J.W., Belser, C.G., 2008. Detection and discrimination of fauna in the aerosphere using Doppler weather surveillance radar. Integr. Comp. Biol. 48, 12–23.
Greenbank, D.O., Schaefer, G.W., Rainey, R.C., 1980. Spruce budworm (Lepidoptera: tortricidae) moth flight and dispersal: new understanding from canopy observations radar, and aircraft. Mem. Ent. Soc. Can. 110, 1–49.
Greenbank, D.O., 1973. The Dispersal Process of Spruce Budworm Moths (Fredericton, NB. Information Report M-X-39. 24 p).
Hennigar, C.R., Erdle, T.A., Gullison, J.J., MacLean, D.A., 2013. Re-examining wood supply in light of future spruce budworm outbreaks: a case study in New Brunswick. For. Chron. 89, 42–53.
Henson, W.R., 1951. Mass flights of the spruce budworm. Can. Entomol. 83, 240.
Horn, J.W., Kunz, T.H., 2008. Analyzing NEXRAD doppler radar images to assess nightly dispersal patterns and population trends in Brazilian free-tailed bats (Tadarida brasiliensis). Integr. Comp. Biol. 48, 24–39.
Joe, P., Lapczak, S., 2002. Evolution of the Canadian operational radar network. Proceedings of the Second European Conference on Radar in Meteorology and Hydrology (ER2002 CE), 370–382.
Kelly, J.F., Shipley, J.R., Chilson, P.B., Howard, K.W., Frick, W.F., Kunz, T.H., 2012. Quantifying animal phenology in the aerosphere at a continental scale using NEXRAD weather radars. Ecosphere 3, 16.
Leskinen, M., Markkula, I., Koistinen, J., Pylkkö, P., Ooperi, S., Siljamo, P., Ojanen, H., Raiskio, S., Tiilikkala, K., 2011. Pest insect immigration warning system by an atmospheric dispersion model: weather radars and traps. J. Appl. Entomol. 135, 55–67.
Ministère des Forêts, de la Faune et des Parcs, 2016. Aires infestées par la tordeuse des bourgeons de l'épinette au Québec en 2016 – Version 1.0, Québec, gouvernement du Québec, Direction de la protection des forêts, 16 p.
Martin, W.J., Shapiro, A., 2007. Discrimination of bird and insect radar echoes in clear air using high-resolution radars. J. Atmos. Oceanic Technol. 24, 1215–1230.
Melnikov, V., Leskinen, M., Koistinen, J., 2014. Doppler velocities at orthogonal polarizations in radar echoes from insects and birds. IEEE Geosci. Remote Sens. Lett. 11, 592–596.
Miller, C.A., Greenbank, D.O., Kettela, E.G., 1978. Estimated egg deposition by invading spruce budworm moths (Lepidoptera: tortricidae). Can. Entomol. 110, 609–615.
Nealis, V.G., Régnière, J., 2004. Insect-host relationships influencing disturbance by the spruce budworm in a boreal mixedwood forest. Can. J. For. Res. 34, 1870–1882.
Nieminen, M., Leskinen, M., Helenius, J., 2000. Doppler radar detection of exceptional mass-migration of aphids into Finland. Int. J. Biometeorol. 44, 172–181.
Peltonen, M., Liebhold, A.M., Bjørnstad, O.N., Williams, D.W., 2002. Spatial synchrony in forest insect outbreaks: roles of regional stochasticity and dispersal. Ecology 83, 3120–3129.
R Core Team, 2016. R: A Language and Environment for Statistical Computing. R Foundation for Statistical Computing, Vienna, Austria https://www.R-project.org/.
Régnière, J., St-Amant, R., 2007. Stochastic simulation of daily air temperature and precipitation from monthly normals in North America north of Mexico. Int. J. Biometeorol. 51, 415–430.
Régnière, J., Delisle, J., Bauce, E., Dupont, A., Therrien, P., Kettela, E., Cadogan, L., Retnakaran, A., van Frankenhuyzen, K., 2001. Understanding of spruce budworm population dynamics: developement of early intervention strategies. Can. For. Serv., 57–70 (Inf. Rep NOR-X-381).
Régnière, J., Delisle, J., Pureswaran, D.S., Trudel, R., 2013. Mate-finding allee effect in spruce budworm population dynamics. Entomol. Exp. Appl. 146, 112–122.
Régnière, J., St-Amant, R., Béchard, A., 2014. BioSIM 10 User's Manual. Natural Resources Canada, Canadian Forest Service, Information Repost LAU-X-137E. URL: http://cfs.nrcan.gc.ca/pubwarehouse/pdfs/34818.pdf (last accessed 14/06/2016).
Rennie, S.J., 2014. Common orientation and layering of migrating insects in southeastern Australia observed with a Doppler weather radar. Meteorol. Appl. 21, 218–229.
Reynolds, D.R., Chapman, J.W., Edwards, A.S., Smith, A.D., Wood, C.R., Barlow, J.F., Woiwod, I.P., 2005. Radar studies of the vertical distribution of insects migrating over southern Britain: the influence of temperature inversions on nocturnal layer concentrations. Bull. Entomol. Res. 95, 259–274.
Reynolds, D.R., Smith, A.D., Chapman, J.W., 2008. A radar study of emigratory flight and layer formation by insects at dawn over southern Britain. Bull. Entomol. Res. 98, 35–52.
Rhainds, M., Brodersen, G., 2012. Wing wear of adult *Choristoneura fumiferana* (Lepidoptera Tortricidae) in relation to age, sex ratio, and presence of host plant. Appl. Entomol. Zool. 47, 475–478.
Rhainds, M., Heard, S.B., 2015. Sampling procedures and adult sex ratios in spruce budworm. Entomol. Exp. Appl. 154, 91–101.
Rhainds, M., 2015. Wing wear and body size measurements of adult spruce budworms captured at light traps: inference on seasonal patterns related to reproduction. Appl. Entomol. Zool. 50, 477–485.
Ruth, J.M., Buler, J.J., Diehl, R.H., Sojda, R.S., 2008. Management and research applications of long-range surveillance radar data for birds, bats, and flying insects. In: U.S. Geological Survey Fact Sheet., pp. 2008–3095.
Schaefer, G.W., 1976. Radar observations of insect flight. In: Rainey, R.C. (Ed.), Insect Flight. Blackwell, Oxford (United Kingdom), pp. 157–197 (Symposia of the Royal Entomological Society no. 7).
Southwood, T.R.E., 1977. Habitat, the templet for ecological strategies? J. Anim. Ecol. 46, 337–365.
Sturtevant, B.R., Achtemeier, G.L., Charney, J.J., Anderson, D.P., Cooke, B.J., Townsend, P.A., 2013. Long-distance dispersal of spruce budworm (*Choristoneura fumiferana*Clemens) in Minnesota (USA) and Ontario (Canada) via the atmospheric pathway. Agric. For. Meteor. 168, 186–200.
Westbrook, J.K., Isard, S.A., 1999. Atmospheric scales of biotic dispersal. Agric. For. Meteorol. 97, 263–274.
Westbrook, J.K., Esquivel, J.F., Lopez Jr., J.D., Jones, G.D., Wolf, W.W., Raulston, J.R., 1998. Validation of bollworm migration across south-central Texas in 1994–1996. S. W. Entomol. 12, 209–219.
Westbrook, J.K., Eyster, R.S., Wolf, W.W., 2014. WSR-88D doppler radar detection of corn earworm moth migration. Int. J. Biometeorol. 58, 931–940.
Wood, C.R., Chapman, J.W., Reynolds, D.R., Barlow, J.F., Smith, A.D., Woiwod, I.P., 2006. The influence of the atmospheric boundary layer on nocturnal layers of noctuids and other moths migrating over southern Britain. Int. J. Biometeorol. 50, 193–204.
Wood, C.R., Reynolds, D.R., Wells, P.M., Barlow, J.F., Woiwod, I.P., Chapman, J.W., 2009. Flight periodicity and the vertical distribution of high-altitude moth migration over southern Britain. Bull. Entomol. Res. 99, 525–535.
Wood, C.R., Clark, S.J., Barlow, J.F., Chapman, J.W., 2010. Layers of nocturnal insect migrants at high-altitude: the influence of atmospheric conditions on their formation. Agric. For. Entomol. 12, 113–121.